Supplementary Information

Innovative strategy with potential to increase hemodialysis efficiency and safety

Hsiao-Chien Chen, Hsiu-Chen Lin, Hsi-Hsien Chen, Fu-Der Mai, Yu-Chuan Liu**, Chun-Mao Lin, Chun-Chao Chang, Hui-Yen Tsai & Chih-Ping Yang

Supplementary Materials

1. Chemicals and materials

Electrolytes of NaCl (99+%) and potassium hexacyanoferrate (III) ($K_3Fe(CN)_6$, 99%) , and creatinine (Crea), hydroquinone (HQ, 99.5%), 5,5-dimethyl-1-pyrroline N-oxide (DMPO) and E. coli lipopolysaccharide (LPS) were purchased from Sigma-Aldrich Organics. Reagents of methylene blue (MB), H_2O_2 and iron(II) chloride tetrahydrate were purchased from Acros Organics. Reagent of blood urine nitrogen (BUN, 99.7%) was purchased from J. T. Baker. Phosphate-buffered saline (PBS) was purchased from Bioman Organics. Ethylenediaminetetraacetic acid (EDTA) was purchased from Bioshop Organics. All of the reagents were used as received without further purification. Dialysis membrane (T1-Series MWCO: 3500) used in MB-related experiments was purchased from Orange (USA). 40 mesh-screened ceramic particles (Molar compositions: 92 % SiO_2, 3.0 % Na_2O and K_2O, 2.0 % Fe_2O_3, 1.5 % Al_2O_3, 0.5 % CaO, 0.5 % MgO, and other rare metal oxides) for filtering through drink water were purchased from Chyuan-Bang enterprise Co., Ltd., Taiwan. Commercial chitosan (Ch) powders with a degree of deacetylation of 0.82 were purchased from First Chemical Works, Taiwan. All of the solutions were prepared using deionized (DI) 18.2 MΩ cm water provided from a Milli-Q system. All of the experiments were performed in an air-conditioned room at ca. 24 ^oC. The water temperature is ca. 23.6 ^oC.

Supplementary Methods

1. Preparation of gold nanoparticles

The Au NPs in an aqueous solution was obtained from an Au sheet (purity of 99.99%) by using electrochemical and thermal reduction methods, as shown in our previous report[33]. Typically, the Au electrode was cycled in a deoxygenated aqueous solution of

40 mL containing 0.1 M NaCl and 1 g L^{-1} Ch from -0.28 to +1.22 V vs Ag/AgCl at 500 mV s^{-1} for 200 scans under slight stirring. The durations at the cathodic and anodic vertices are 10 and 5 s, respectively. Immediately, without changing the electrolytes, the solution was heated from room temperature to boiling at a heating rate of 6 ^{o}C min^{-1} in air. After cooling the clear Au NPs-containing solution was separated from the settlement of Ch. Then the Au NPs-containing solution was placed in an ultrasonic bath for 30 min and was further centrifuged at 3600 rpm for 2 min to remove Ch for preparing pure Au NPs in solution.

2. Preparation of ceramic particles-supported Au NPs

The rinsed ceramic particles were immersed in a solution containing 30 ppm Au NPs for 1 day. Then the Au NPs-adsorbed ceramic particles were rinsed throughout with deionized water, and finally dried in an oven at 100 ^{o}C for 1 day. Subsequently, the prepared Au NPs-adsorbed ceramic particles were loaded in a valve-equipped glass tube (I.D.: 15 mm, L: 550 mm). Before prepare the AuNT water the ceramic particles-supported Au NPs in the glass tube were rinsed with deionized water for several cycles until the pH values of deionized water before and after it passed through the particle-loaded tube are almost identical (ca. pH 7.26 and water temp. at ca. 23.6 ^{o}C).

3. UV-vis spectrum of ceramic particles-supported Au NPs

Ultraviolet-visible absorption measurements for the ceramic particles-supported Au NPs was carried out by using a Perkin-Elmer Lambda 800/900 spectrophotometer. For measuring the spectrum of the solid ceramic particles-supported Au NPs based on a reflection model the spectrophotometer was equipped with a collector of integrating sphere. Wetted ceramic particles were used as the background reference in experiment.

4. Preparation conditions of AuNT water

In preparations deionized (DI) water (pH 7.26, T = 23.6 ^{o}C) flowed through the glass tube filled with Au NPs-adsorbed ceramic particles under illumination. Then the AuNT water (pH 7.25, T = 23.4 ^{o}C) was collected in glass sample bottles for subsequent tests as soon as possible. For examining the purity of the prepared AuNT water further inductively coupled plasma-mass spectrometer (ICP-MS) analyses indicated that the concentrations of the slightly dissolved metals in the AuNT water are ca. 0.60, 33, 21, 19, 11, 3.6 and 0.36 ppb for Au, Na, K, Al, Mg, Ca and Fe, respectively. Excluding Au, the total equivalent molar concentration of these dissolved metals is equal to ca. 5.2×10^{-6} N. This measured value is ca. 2.4×10^{-7} N

for DI water as a reference.

5. Raman spectra recorded on water and their deconvolutions

In measurement prepared water was sealed in a 0.5 mL cell with glass window. Raman spectra were recorded (Micro Raman spectrometer, Model RAMaker) by using a confocal microscope employing a DPSS laser operating at 532 nm with an output power of 1 mW on the sample. A 50x, 0.36 NA Olympus objective (with a working distance of 10 mm) was used to focus the laser light on the samples. The laser spot size is ca. 2.5 μm. A thermoelectrically cooled Andor iDus charge-coupled device (CCD) 1024 x 128 pixels operating at -40 ^{o}C was used as the detector with 1 cm^{-1} resolution. All spectra were calibrated with respect to silicon wafer at 520 cm^{-1}. In measurements, a 90^{o} geometry was used to collect the scattered radiation. A 325 notch filter was used to filter the excitation line from the collected light. The acquisition time for each measurement was 1 s. Thirty sequential measurements were collected for each sample. These Raman spectra were further deconvoluted into five Gaussian sub-bands based on the methods shown in the literature[25,26,34]. In deconvolution the five-Gaussian components with the center wavenumbers at 3018, 3223, 3393, 3506 and 3624 cm^{-1} were adopted for all samples. Moreover, the full width at half maximum (FWHM) of the individual component in the five-Gaussian fit was equal for all samples. These values are 234, 201, 176, 145 and 112 cm^{-1} for bands at 3018, 3223, 3393, 3506 and 3624 cm^{-1}, respectively. The qualities of these fitted spectra are satisfactory.

6. Chemical activity of water in reduction preparation of Au nanoparticles

First, ca. 500 ppm Au-containing complex was electrochemically prepared in DI water by using the similar method shown in a previous report[35]. Typically in preparation of Au-containing complex, the Au electrode was cycled in a deoxygenated aqueous solution containing 1 N NaCl from -0.28 V (holding 10 s) to 1.22 V (holding 5 s) at 500 mV s^{-1} for 500 scans. Then 8 mL DI water or sAuNT water was mixed with 2 mL of the prepared Au complex-containing solution in a glass sample cell (20 mL). The final concentration of the Au-containing complex in solution was 100 ppm. Subsequently, 40 mesh-screened ceramic particles (ca. 5 mL) was added in the mixed solution for nucleation of Au NPs from the sAuNT water-assisted reduction of the Au-containing complexes. Immediately, the samples were sealed and placed in ambient laboratory air and in dark for further observation.

7. Simulated HD experiments and concentration measurements of BUN and Crea

In HD experiments, hollow fiber dialyzers with polymethylmethacrylate (PMMA)

membranes (model: B3-1.0A, Toray Filtryzer, Japan) were employed. The blood with high concentrations of BUN (ca. 100 mg dL^{-1}) and Crea (ca. 20 mg dL^{-1}) flowed into the dialyzer from the top entrance and out from the bottom exit. The dialysate based on sAuNT water (or based on DI water) flowed into the dialyzer from the bottom entrance and from the top exit. The flowing mode of these two streams is of countercurrent. Before experiments, suitable quantities of BUN and Crea (estimation by deducting the originally normal values in blood) were added in blood to prepare blood sample with required 100 mg dL^{-1} BUN and 20 mg dL^{-1} Crea under stirring without destroying the structure of blood. Then the blood sample was evenly divided into two parts for being individually dialyzed by using dialysates based on saline solution (DI) and on saline solution (sAuNT). The osmolarities (measured from Osmometer, model 3250) are 278, 286 and 290 mosmol L^{-1} for dialysates based on saline solution (DI), saline solution (AuNT) and saline solution (sAuNT), respectively.

The concentrations of BUN and CREA in dialyzed bloods were analyzed as follows. BUN was tested by kinetic UV assay (cobas); while Crea was tested by picric acid jaffe method (cobas). All analyses work on Roche automated clinical chemistry analyzers modular (Modular P800, Roche Diagnostics, Indianapolis, US).

8. Measurement of hydroxyl free radicals by electron spin resonance spectroscopy

In electron spin resonance (ESR) measurement, a Bruker EMX ESR spectrometer was employed. ESR spectra were recorded at room temperature using a quartz flat cell designed for solutions. The dead time between sample preparation and ESR analysis was exactly 1.5 min after the last addition. Conditions of ESR spectrometry were as follows: 20 mW power at 9.78 GHz, with a scan range of 100 G and a receiver gain of 6.32×10^4.

9. Sample preparation for measuring hydroxyl free radicals

The hydroxyl free radicals were obtained by using the well-known Fenton reaction, in which ferrous iron donates an electron to hydrogen peroxide to produce the hydroxyl free radical[36,37]. Because the produced hydroxyl free radicals are very unstable they are capped by spin-trapping using DMPO to form more stable complex radicals for exact detection. The sample preparation is described as follows.

First, 140 μL DI water with 0.9 wt% NaCl or AuNT water with 0.9 wt% NaCl was added in a microtube (Eppendorf). Then 20 μL PBS (10X) was added in the tube. A complex of EDTA-chelated iron(II) was prepared by mixing 0.5 mM iron(II) chloride tetrahydrate and 0.5 mM EDTA with equal volume. Subsequently, 20 μL EDTA-chelated iron(II) (0.25 mM), 10 μL H_2O_2 (0.2 mM) and 10 μL DMPO (2 M)

were sequentially added in the tube. The final volume in the tube is 200 μL. Exact 1.5 min later from the addition of DMPO ESR analysis was performed. To obtain an ESR spectrum, sample was scanned for ca. 1.5 min, accumulated 8 times, and all signals were averaged.

10. Lipopolysaccharide-induced nitric oxide release in culture medium

Determination of nitric oxide (NO) production was made following the method shown in the literature[38]. DI water, AuNT water and sAuNT water were used for medium preparation. RAW 264.7 cells, a murine macrophage cell line, were obtained from American Type Culture Collection (ATCC) and cultured at 37 °C in Dulbecco's Modified Essential Medium supplemented with 10% fetal bovine serum (FBS), 100 units mL^{-1} penicillin, 100 μg mL^{-1} streptomycin, and 5% CO_2 in incubation chamber as recommended by ATCC. Briefly, RAW 264.7 cells grown on a 10 cm culture dish were seeded in 96-well plates at a density of 2×10^5 cells/well. Adhered cells were then stimulated with various concentrations (0-100 ng mL^{-1}) of E. coli LPS for 24 h. Nitrite in culture medium was measured by adding 100 μL of Griess reagent (1% sulfanilamide and 0.1% N-[1-naphthyl]-ethylenediamine dihydrochloride in 5% phosphoric acid) to 100 μL samples of the medium for 10 min at room temperature. The optical density at 570 nm was measured using a Multiskan RC photometric microplate reader (Labsystems, Helsinki, Finland). A NO standard curve was made with sodium nitrite. The levels of NO production were normalized to cell viability.

Supplementary Discussion

1. DNHBWs on differently treated water

As demonstrated in Table S1, the AuNT water obtained without illumination of light was obtained by using a similar preparation condition used for the preparation of AuNT water or sAuNT water, but without illumination of fluorescent lamps or green LED. The Raman spectrum of super sAuNT water was obtained by irradiating sAuNT water-wetted ceramic supported Au NPs with laser light at 532 nm. The close values of 21.29 and 21.41 % for the DI water and the AuNT water obtained without illumination of light show that AuNT water can't be obtained by just using supported Au NPs in the absence of the LSPR effect from the resonant lights. The DNHBW of super sAuNT water is 30.80 %, which is far higher than the value of sAuNT water. To consider the effect of temperature, a similar experiment was performed by using the similar preparation condition used for the preparation of the super sAuNT water, but DI water was used to wet the Au NPs-free ceramic particles. The obtained DNHBW was ca. 21.83 %. It suggests that the temperature effect only exerts a slight influence on the observed extremely high DNHBW of the super sAuNT water. Also, no asymmetric stretching vibration of the isolated water molecule was observed at ca. 3755 cm^{-1}, suggesting that water vapor can be excluded from this super sAuNT water [39]. Ag NPs instead of Au NPs were also employed in the preparation of AuNT water under illuminations of green and blue LED. The results also support the idea in the preparation of AuNT water by using the LSPR effect from the irradiated Au or Ag NPs. The values of DNHBW are 22.38 and 26.13 % based on Ag NPs irradiated by non-maximum-resonant green LED (maxima centered at 530 nm) and by exactly resonant blue LED (maxima centered at 460 nm), respectively.

2. Energy efficiency analysis on preparation of small water clusters

The energy efficiency, η, in the preparation of AuNT water under illumination of green LED was estimated from the ratio of the energy required for breaking the hydrogen bonds in bulk water to that provided from the light energy of LED, as defined below.

$$\eta = (E_{HB}M_{water}) / (P_{LED}t) \times 100\ \%$$

where energy of hydrogen bond, E_{HB}, of 20 kJ mol^{-1} was used. For obtaining 75 g (or 75 cm^3, as using density of 1 g cm^{-3}) AuNT water the moles of bulk water, M_{water}, in which hydrogen bonds were broken, were calculated from the moles (4.2 mol) multiplied by the difference of DNHBW of DI water (21.29 %) and sAuNT water

(26.78 %) under illumination of green LED. The used power of LED, P_{LED}, was 16 W and the illumination time, t, for 75 cm^3 DI water passing through the glass tube was ca. 1500 s. Therefore, the energy efficiency for preparing AuNT water under illumination of green LED is approximately 4.6 kJ/24 kJ = 19% in ignorance of energy losses from scattering of LED and penetrating glass tube of light.

3. Mechanism on formation of AuNT water with weak hydrogen bonds and its corresponding persistence in liquid water

As reported in the literature[22,23,40], light-induced vapor generation at water-immersed Au NPs was enabled when Au NPs were illuminated with solar energy or resonant light of sufficient intensity. However, the threshold of resonant light intensity is (~10^6 W m^{-2}). In this work, in preparation of AuNT water with weak hydrogen bonding DI water (pH 7.26, T = 23.6 ^oC) flew through the glass tube (diameter of 15 cm) filled with Au NPs-adsorbed ceramic particles (height of 45 cm) under illumination. Then the AuNT water (pH 7.25, T = 23.4 ^oC) was collected in glass sample bottles for subsequent tests as soon as possible. In illuminations with full visible wavelength fluorescent lamp, or alternatively green LED (wavelength maxima centered at 530 nm) the light power density at resonant 540 nm is ca. 10^{-3} W m^{-2}, or 10^{-2} W m^{-2}, respectively, which is far lower than that of the required threshold for light-induced vapor generation. In more detailed comparison, time for the water steam generation in the batch system is less 5 s after illumination commenced[22]. In our continuous system, the time for water flowing through the glass tube is ca. 1500 s. The energy density used in this work is still far lower than that for generating water steam shown in the literature. It is well known that required heat is 10~40 KJ mol^{-1} for breaking the hydrogen bond, which is lower than that of 136 KJ mol^{-1} for evaporating water at room temperature. In this work, the water temperature wasn't significantly changed when it flew through the glass tube with Au NPs under illumination. Therefore, the effect of light-to-heat conversion for breaking the hydrogen bonds of bulk water can be achieved under illumination with full-wavelength visible light and further enhanced by wavelength optimized resonant light.

Meanwhile, measured DNHBW values of 27.66, 27.29, 26.73, and 25.62 % were recorded, for saline solution (sAuNT water), after 0, 2, 4 and 7 days, respectively. The slow rate of decay for prepared AuNT water is not contrast to the time scale (~ 10^{-12} s) normally ascribed to hydrogen bond breaking and reformation in water. Because the forward reaction from bulk water to AuNT water with weak hydrogen bonds is endothermic the light-to-heat conversion from the Au NPs under resonant illumination favors this forward reaction. In storage in absence of Au NPs, both the forward and reverse reactions are slow due to huge activation energies required for both reactions.

In this work, the values of DNHBW are all located on the level of 26 % for AuNT water prepared by using NPs of Au and Ag under illuminations of resonant green and blue LED, respectively, as demonstrated in Table S1. The different NPs should be responsible for distinguishable resonant effects under the similarly resonant illuminations, but the prepared AuNT water owns the similar DNHBW. It strongly suggests that the prepared AuNT water with a higher energy, compared to bulk water, is trapped in a relatively stable state in an activation energy valley, in which in absence of catalytic Au NPs it can persist in liquid water without reverting to normal hydrogen-bonding patterns observed in bulk water. However, the hydrogen-bond network is still constantly evolving with the same time scale.

4. Diffusion coefficient of $K_3Fe(CN)_6$ and HQ in water

The diffusion coefficients of $K_3Fe(CN)_6$ (or HQ) in saline solutions can be calculated according to the well-known Randles-Sevcik equation[41].

$$I_{pa} = 2.69 \times 10^5 \, AD^{1/2} n^{3/2} v^{1/2} C \qquad (1)$$

where A represents the area of the electrode (7.07 cm^2 for used Pt electrode), n the number of electrons participating in the reaction, and is equal to 1 (2 for HQ), C the concentration of the probe molecule in the solution, and is 3×10^{-5} (1×10^{-6} for HQ) mol cm^{-3}, and v is the scan rate (0.1 V s^{-1}). The I_{pa} (A) refers to the anodic peak current shown in Fig. 2 (main text). Then the diffusion coefficient D of the dissolved molecule in saline solution can be obtained.

Moreover, in NaCl-free aqueous solution, the calculated diffusion coefficient of $K_3Fe(CN)_6$ increased from 1.36 to 2.02×10^{-6} cm s^{-1} when using AuNT water instead of conventional DI water. This is an increase of 49 % for the diffusion coefficient. This increased to 82 % using AuNT water prepared using green LED illumination (2.48×10^{-6} cm s^{-1})

5. Chemical activity of AuNT water in reduction

As shown in Fig. S2 (a), the absorbance maximum band of the electrochemically prepared Au-containing complexes (yellow in solution) appears at ca. 310 nm. These absorbance maximum bands are unchanged and still appear at ca. 309 nm when the Au-containing complexes are initially added in both sAuNT water and DI water with ceramic particles, as shown in Figs. S2 (b) and (c). After experiments for 5 days, this absorbance band disappears for the sAuNT water-containing sample (Fig. S2 (d)); while it still appears at ca. 304 nm for DI water-containing sample (Fig. S2 (e)). Encouragingly, at the same time, the color of the originally white ceramic particles

(pale yellow in adsorption of yellow Au-containing complexes) in the AuNT water-containing solution became red (a characteristic color of Au NPs), as demonstrated in Fig. S3 (a); while the color of ceramic particles is still unchanged in the DI water-containing solution, as demonstrated in Fig. S3 (b). To further confirm the successful preparation of Au NPs by using sAuNT water as reducing reagent, the Au NPs-adsorbed ceramic particles and the Au NPs-free ceramic particles, as discussed above, were rinsed throughout with DI water. Subsequently, ultrasonic treatments were performed by putting them in an ultrasonic bath for 15 min to obtain Au NPs-containing and Au NPs-free solutions. Then UV-vis absorption spectra were measured and shown in Figs. S2 (f) and (g). The absorbance maximum band of the solution appears at ca. 545 nm, as shown in Fig. S2 (f). It indicates that the Au NPs have been successfully prepared[42] under the assistance of reducing agent of sAuNT water. However, there is no absorbance maximum band in the solution regarding with Au NPs, as shown in Fig. S2 (g) based on inert DI water. As reported by Vohringer-Martinez et al.[43], radical-molecule gas-phase reaction could be catalyzed by water molecules through their ability to form hydrogen bonds. Small gas-phase water clusters could bind an excess electron through a double hydrogen-bond acceptor motif[44]. However, this novelty chemical activity of liquid water is less discussed in the literature. It opens a new green pathway in chemical reduction. We think more free water available in the AuNT water with weaker hydrogen bonding should be responsible for this novelty activity.

6. Scavenging ability of AuNT water on hydroxyl free radicals

As shown in Fig. S4, the four splitting signals are the characteristics of hydroxyl radicals[36]. The Fenton reaction-produced hydroxyl radicals were reduced in the presence of prepared AuNT water in saline solution, as compared to saline solution (DI). The corresponding ESR intensities were decreased by ca. 7.3 and 9.4 % in saline solution (AuNT) and saline solution (sAuNT), respectively, as compared with that for an experiment performed in saline solution (DI). In calculating the average intensities the two strongest peaks at ca. 3471 and 3486 G were used. The detailed data were also demonstrated in Table S2. As shown in the literature[45,46], water can form an H_2O-OH radical complex through hydrogen bonding in the atmosphere. To the best of our knowledge, this anti-oxidative activity by scavenging free radicals from AuNT or sAuNT liquid water is the first report in the literature.

7. Anti-oxidative activity of AuNT water on reduction of LPS-induced NO release

As reported by Ohsawa et al.[36], acute oxidative stress, induced by inflammation, causes serious damage to tissues, while persistent oxidative stress is an acknowledged

underlying cause of many common diseases, including cancer[47]. Their studies indicated that hydrogen can selectively reduce the hydroxyl radical, the most cytotoxic reactive oxygen species (ROS), but that hydrogen did not react with other ROS. Because intracellular ROS level is closely associated with NO production in macrophage cells, AuNT water or sAuNT water with anti-oxidative activity *in vitro* prompted an experiment to determine the activity in cells. Stimulating macrophages with LPS caused a gradual nitrite release in cell culture medium with a dose-dependent manner. Nitrite monitoring was performed using the Griess reaction as isolated measurements at 24 h after the stimulation by LPS. The same experiments using cells with LPS stimulation were performed as ROS level indication. In order to evaluate the effects of AuNT water and sAuNT water on activated macrophage cells, AuNT water, sAuNT water and DI water-prepared Dulbecco's Modified Essential Medium (DMEM) were compared for RAW 264.7 macrophage cells culture with LPS stimulation (0-100 ng mL^{-1}). As shown in Fig. 3 (main text), the NO production that stimulates macrophages with LPS was lower in AuNT water prepared medium, especially lower in sAuNT water prepared medium, when compared to control DMEM medium. The elevated NO production levels were significantly decreased ($p<0.05$) in AuNT water (especially in sAuNT water prepared under LED illumination) DMEM in the presence of LPS from 10 to 100 ng mL^{-1}. Incubation with prepared AuNT water-DMEM gives rise to suppression of NO release in LPS-activated macrophage cells.

8. Diffusion experiments of MB in differently treated water

Figure S5 (a) shows the experimental setup used in diffusion experiments of MB in different water. At beginning, 0.3 mM MB was dissolved in water at the left side of the double-cylinder glass cell, which was separated by a dialysis membrane. The right side of the glass cell is a dialysate of pure water without NB. The absorbance intensity of percolated MB in dialysate was recorded with time by using a UV-vis absorption spectrometer at 665 nm. As shown in Fig. S5 (b), MB was initially dissolved in DI water (or in AuNT water or in sAuNT water); while the used dialysate is the same DI water without MB for the whole three-set experiments. After experiment for 3 h, the absorbance intensities of MB, which is corresponding to its concentration, can be increased by 55 % (16 % for 6 h) and 100 % (44 % for 6 h) by utilizing AuNT water and sAuNT water, respectively, instead of DI water in the system. As shown in Fig. S5 (c), MB was also initially dissolved in DI water (or in AuNT water or in sAuNT water); while the used dialysate is corresponding to DI water (or to AuNT water or to sAuNT water), respectively, without MB for the whole three-set experiments. After experiment for 3 h, the absorbance intensities of MB can be increased by 69 % (28 % for 6 h) and 135 % (82 % for 6 h) by utilizing AuNT water and sAuNT water,

respectively, instead of DI water in the system. There are three noticeably interesting phenomena revealed in Figs. S5 (b) and (c). One is the maximum increased degrees of the increased absorbance intensities of MB appear at the middles of experiments for ca. 3 h in both AuNT water and sAuNT water systems. Then these increased degrees of the increased absorbance intensities of MB are gradually decreased with time. The reason can be ascribed to the gradual decrease in concentration difference of MB with time in AuNT water system, especially in sAuNT water system, as compared to in DI water system. Another is the increased degree of the increased absorbance intensity of MB is more significant in sAuNT water system than in AuNT water system, which can be ascribed to the higher diffusion coefficient of sAuNT water than that of AuNT water. The other is the increased degree of the increased absorbance intensity of MB is more significant in double-side-containing AuNT (or sAuNT) water system than in one-side-containing AuNT (or sAuNT) water system. This suggests that more efficient diffusion of solutes can be achieved when AuNT water is present in both dialyzed solution and dialysate.

9. Simulated HD experiments based on two other blood samples and water-based sample

The treatment time was recorded after the first droplet of dialysate flew through the dialysate output. The used dialyzer is also practically employed in hospital. As shown in Figs. S6 (a) and (b) based on another blood sample, which is different from that shown in Fig. 4 (main text), the treatment times for removals of 70 % BUN (100 mg dL^{-1}) in bloods are ca. 19 and 8.9 min by using saline solution (DI) and using saline solution (sAuNT), respectively. The treatment times for removals of 70 % Crea (20 mg dL^{-1}) in bloods are ca. 16 and 5.0 min by using saline solution (DI) and using saline solution (sAuNT), respectively. These results suggest that the treatment times for removals of 70 % BUN and Crea can be markedly reduced by 53 and 69 %, respectively, by utilizing AuNT water instead of DI water in dialysate of saline solution. Also, as shown in Figs. S7 (a) and (b) based on the other blood sample, which is different from that shown in Fig. 4 (main text), the treatment times for removals of 70 % BUN (100 mg dL^{-1}) in bloods are ca. 9.4 and 5.0 min by using saline solution (DI) and using saline solution (sAuNT), respectively. The treatment times for removals of 70 % Crea (20 mg dL^{-1}) in bloods are ca. 7.1 and 4.8 min by using saline solution (DI) and using saline solution (sAuNT), respectively. These results suggest that the treatment times for removals of 70 % BUN and Crea can be markedly reduced by 47 and 32 %, respectively, by utilizing AuNT water instead of DI water in dialysate of saline solution.

Before HD experiments based on water sample, DI water containing BUN and

Crea was dialyzed instead of BUN and Crea-containing blood by using saline solution (DI) and saline solution (AuNT). As shown in Fig. S8 based on BUN (60 mg dL^{-1}) and Crea (15 mg dL^{-1})-containing DI water sample, at the end of experiment for 90 min, the efficiencies for removals of BUN and Crea are markedly increased by 79 and 38 %, respectively, by utilizing AuNT water instead of DI water in dialysate of saline solution.

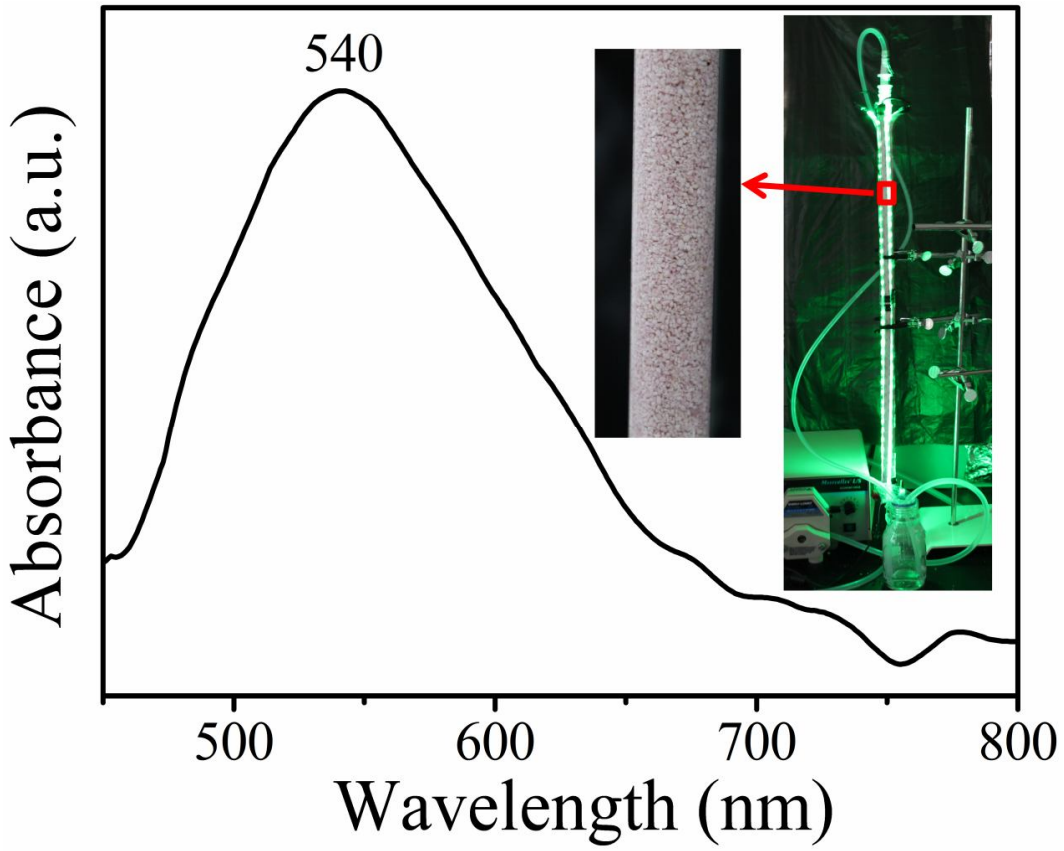

Figure S1 | UV-vis absorption spectrum of ceramic particles-supported Au NPs in solution. Insert showing the glass tube filled with supported Au NPs for the preparation of sAuNT water under illumination of green LED.

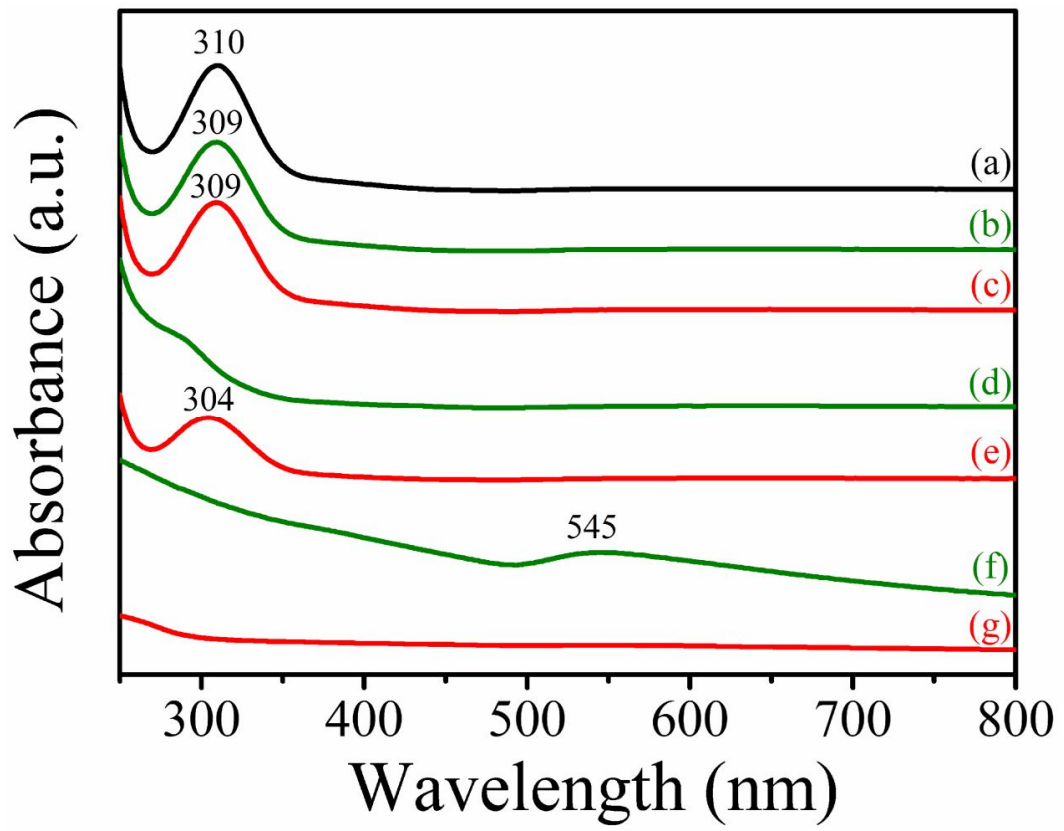

Figure S2 | Time-dependent UV-vis absorption spectra of precursors (black line) of Au NPs and prepared Au NPs in presences of sAuNT (green line) water and DI water (red line) for reference. a, Au salts of precursors of Au NPs. **b**, Au salts of precursors in sAuNT water for 0 day. **c**, Au salts of precursors in DI water for 0 day. **d**, Au salts of precursors in sAuNT water for 5 days. **e**, Au salts of precursors in DI water for 5 days. **f**, Obtained Au NPs in presence of sAuNT water after experiment for 5 days. **g**, None Au NPs obtained in presence of DI water after experiment for 5 days.

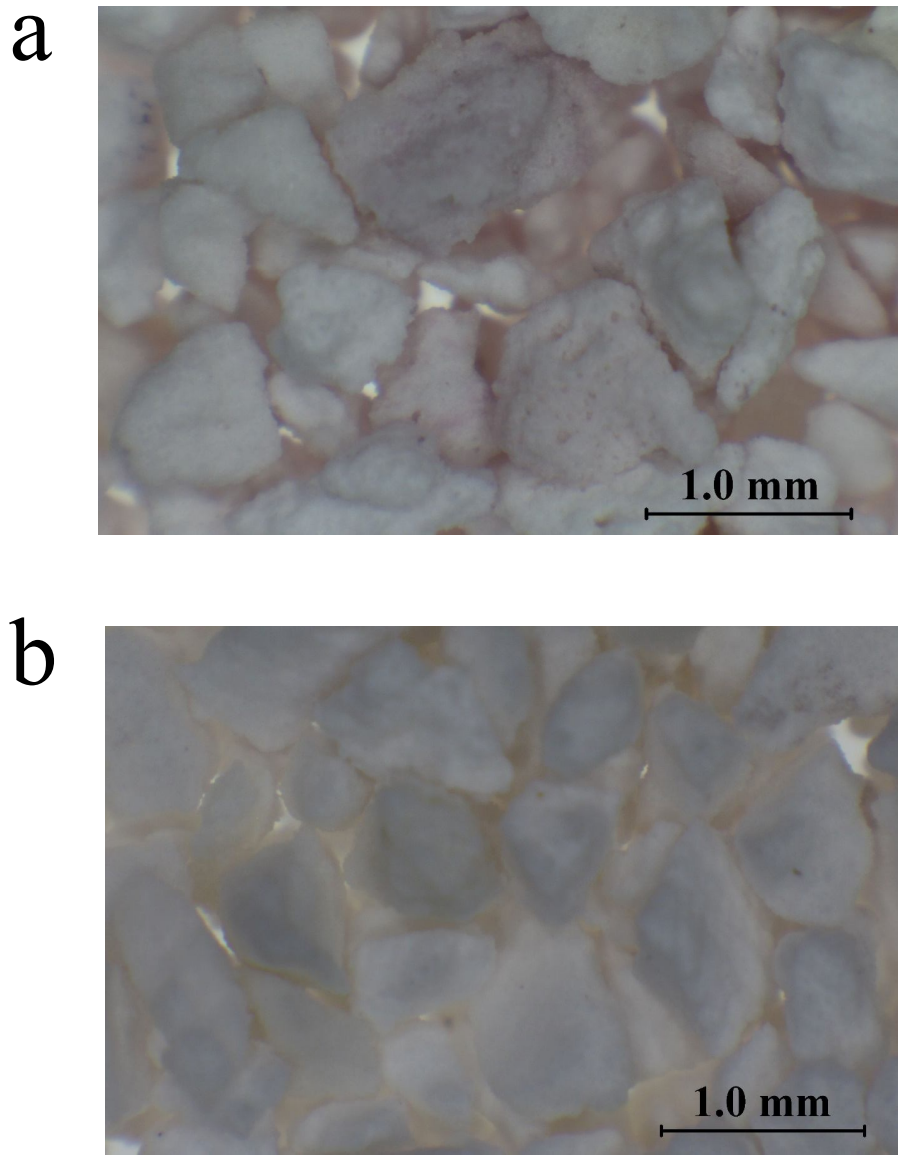

Figure S3 | Optical microscope images showing reduction preparation of Au NPs in presences of sAuNT water and DI water for reference, corresponding to Fig. S2. a, Obtained Au NPs (pale red) in presence of sAuNT water as reducing agent after experiment for 5 days. **b**, None Au NPs obtained in presence of DI water after experiment for 5 days.

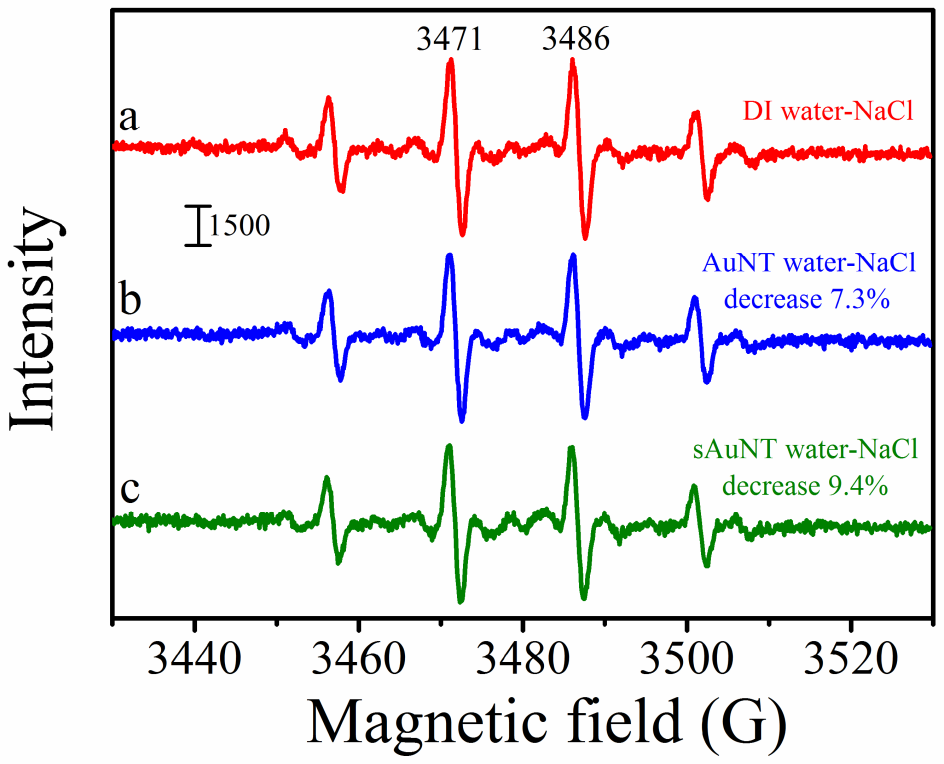

Figure S4 | ESR spectra of hydroxyl free radicals based on various saline solutions. a, Saline solution based on DI water for reference. **b**, Saline solution based on AuNT water prepared under illumination with fluorescent lamps. **c**, Saline solution based on sAuNT water prepared under illumination with green LED. The hydroxyl free radicals were obtained by using the well-known Fenton reaction, in which ferrous iron donates an electron to hydrogen peroxide to produce the hydroxyl free radical.

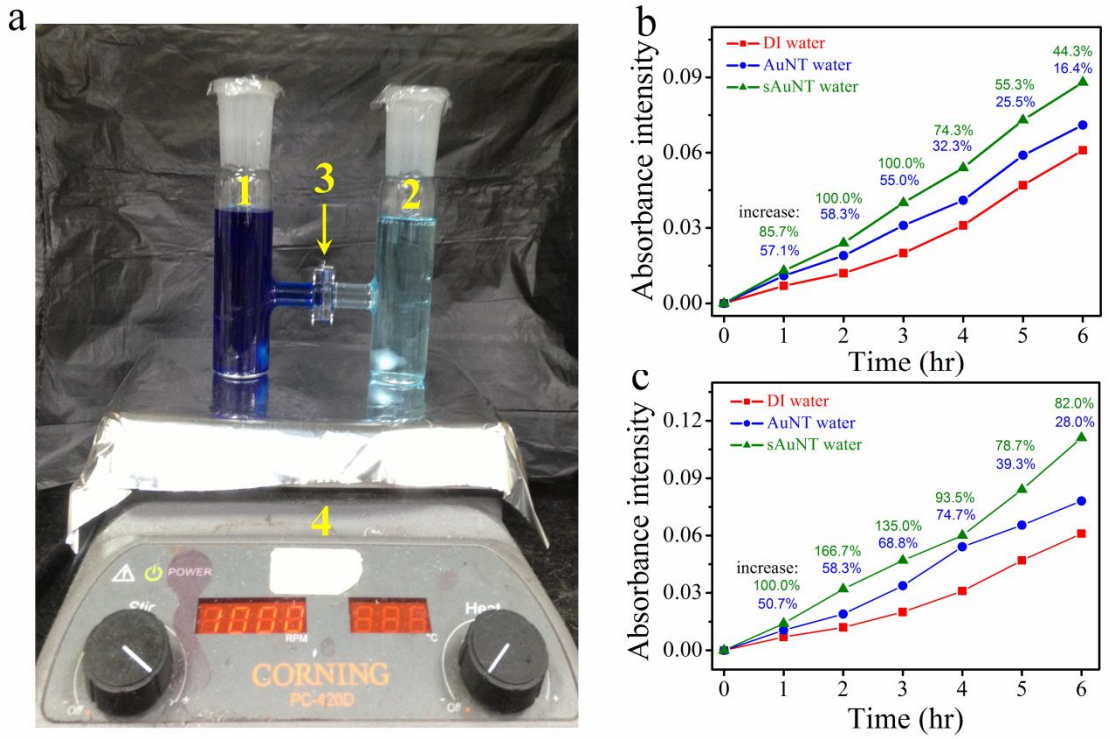

Figure S5 | Equipment in MB diffusion experiments and diffusion efficiencies of MB by using differently treated water. a, Equipment in MB diffusion experiments. 1: 0.3 mM MB in different water (50 mL); 2: dialysate of different pure water (50 mL); 3: dialysis membrane; 4: magnetic stirrer. Both 50 mL samples in 1 and 2 were stirred at 1000 rpm in the whole experiment to homogenize the concentration of sample. The absorbance intensity of percolated MB in dialysate was recorded with time by using a UV-vis absorption spectrometer at 665 nm. **b**, Diffusion efficiencies of MB by using different pure water (type I). Initially, 0.3 mM MB was dissolved in DI water (or in AuNT water or in sAuNT water). The used dialysate is DI water without MB for the whole three-set experiments. **c**, Diffusion efficiencies of MB by using different pure water (type II). Initially, 0.3 mM MB was dissolved in DI water (or in AuNT water or in sAuNT water); while the used dialysate is corresponding to DI water (or to AuNT water or to sAuNT water), respectively, without MB for the whole three-set experiments.

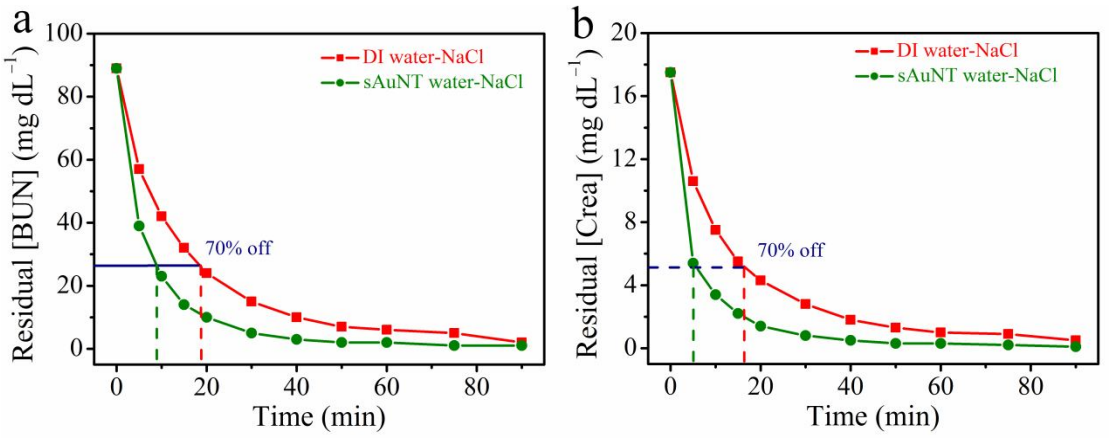

Figure S6 | Removal efficiencies of BUN and Crea by using saline solutions based on different water. The HD experiment was performed by using the similar equipment and method, as shown in Fig. 4 (main text), but by using another blood sample. a, Removal efficiencies of BUN by using different saline solutions. Treatment times for removals of 70 % BUN (initially ca. 100 mg dL^{-1}) are ca. 19 and 8.9 min by using saline solution (DI) and using saline solution (sAuNT), respectively. **b**, Removal efficiencies of Crea by using different saline solutions. Treatment times for removals of 70 % Crea (initially ca. 20 mg dL^{-1}) are ca. 16 and 5.0 min by using saline solution (DI) and using saline solution (sAuNT), respectively.

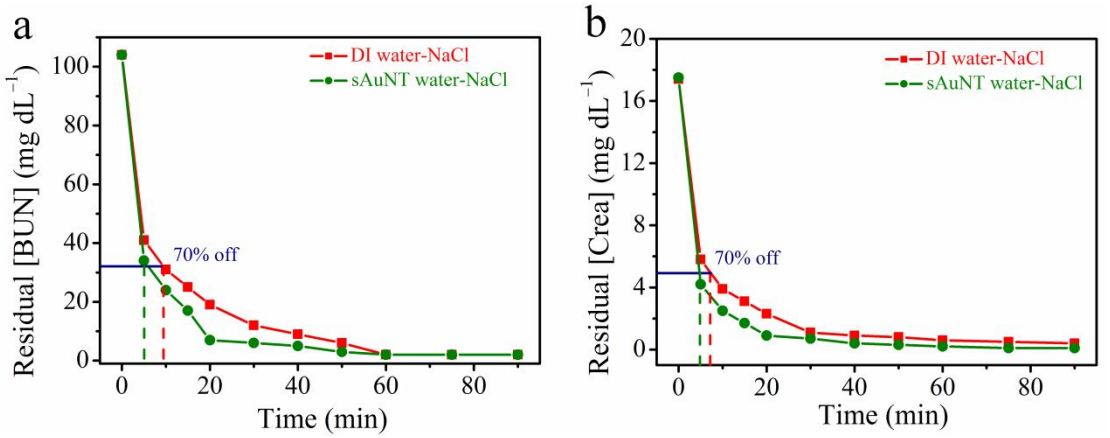

Figure S7 | Removal efficiencies of BUN and Crea by using saline solutions based on different water. The HD experiment was performed by using the similar equipment and method, as shown in Fig. 4 (main text), but by using the other blood sample. a, Removal efficiencies of BUN by using different saline solutions. Treatment times for removals of 70 % BUN (initially ca. 100 mg dL^{-1}) are ca. 9.4 and 5.0 min by using saline solution (DI) and using saline solution (sAuNT), respectively. **b**, Removal efficiencies of Crea by using different saline solutions. Treatment times for removals of 70 % Crea (initially ca. 20 mg dL^{-1}) are ca. 7.1 and 4.8 min by using saline solution (DI) and using saline solution (sAuNT), respectively.

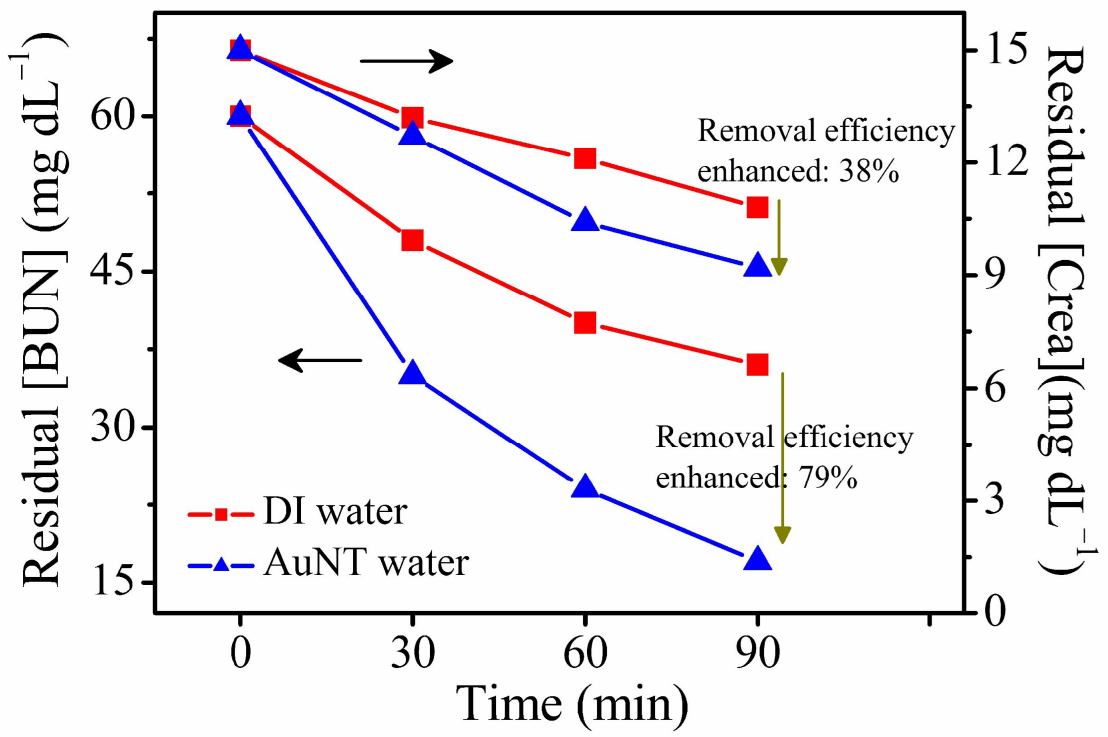

Figure S8 | Removal efficiencies of BUN and Crea by using saline solutions based on different water. The HD experiment was performed by using the similar equipment and method, as shown in Fig. 4 (main text), but by using BUN (ca. 60 mg dL^{-1}) and Crea (ca. 15 mg dL^{-1})-containing DI water sample instead of BUN and Crea-containing blood sample. Both the flow rates of BUN and Crea-containing DI water and dialysate were kept at 24 mL min^{-1} by variable-speed tubing pump. The 1000 mL sample of BUN and Crea-containing DI water was stirred at 200 rpm in the whole experiment to homogenize the concentration of sample. At the end of experiment for 90 min, the residual concentrations of BUN in dialyzed water sample are ca. 36 mg dL^{-1} (10.8 mg dL^{-1} for Crea) and 17 mg dL^{-1} (9.2 mg dL^{-1} for Crea) by using dialysate of saline solution (DI) and using dialysate of saline solution (AuNT), respectively.

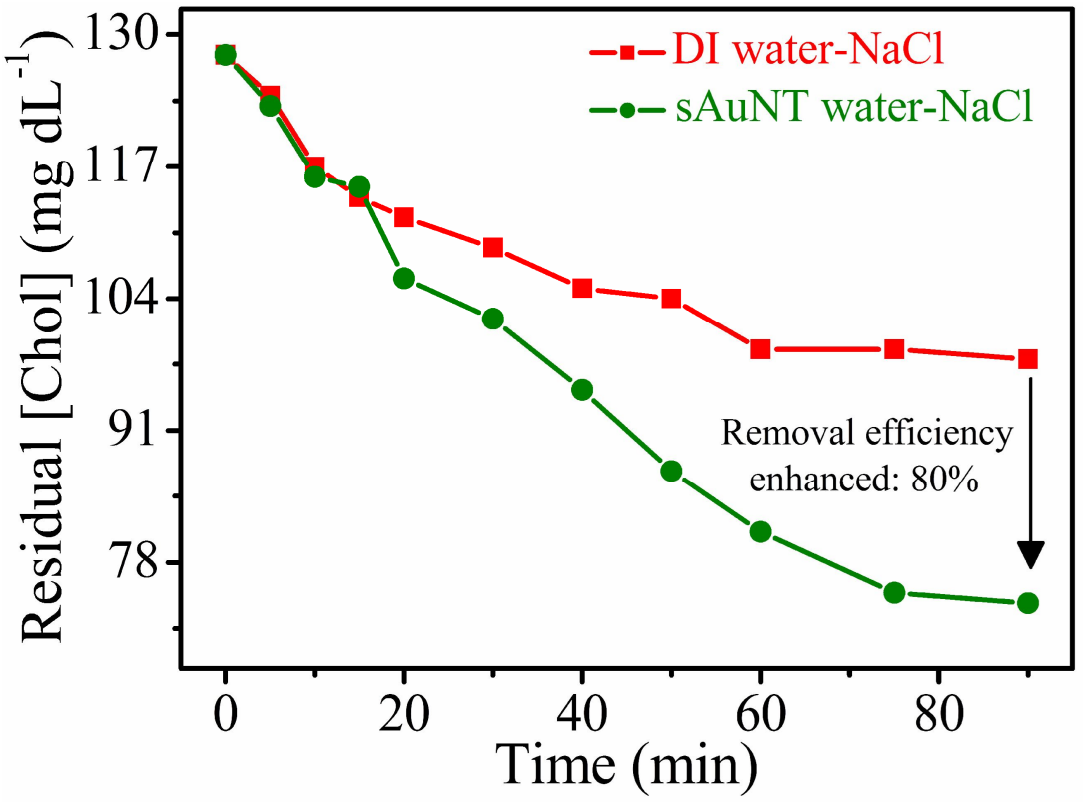

Figure S9 | Removal efficiencies of Cholesterol (Chol) by using saline solutions based on different water. This is the same experiment as the HD experiment, as shown in Fig. 4 (main text), but the residual concentrations of Chol in bloods were measured. At the end of experiment for 90 min, the residual concentrations of Chol in bloods were ca. 98 mg dL^{-1} and 74 mg dL^{-1} by using dialysate of saline solution (DI) and using dialysate of saline solution (sAuNT), respectively. The efficiency for removal of Chol (originally ca. 128 mg dL^{-1}) is markedly enhanced by ca. 80 %, by utilizing AuNT water (sAuNT water) instead of DI water in dialysate of saline solution.

Table S1 | Ratios of five-Gaussian components of OH stretching Raman bands and degree of nonhydrogen-bonded water (DNHBW) in various pure water and saline solutions.

Sample	(1) 3018 cm^{-1} (%)	(2) 3223 cm^{-1} (%)	(3) 3393 cm^{-1} (%)	(4) 3506 cm^{-1} (%)	(5) 3624 cm^{-1} (%)	DNHBW (%)
a	5.77	36.44	36.5	16.25	5.04	21.29
b	3.42	38.34	33.17	18.11	6.96	25.07
c	3.46	36.74	33.02	19.24	7.54	26.78
d	4.69	37.73	33.59	17.15	6.83	23.98
e	3.66	34.50	35.85	18.67	7.32	26.00
f	3.00	35.89	33.44	19.89	7.77	27.66
g	6.02	36.92	35.65	17.09	4.32	21.41
h	2.39	32.24	34.57	21.08	9.72	30.80
i	5.38	35.93	36.31	17.26	5.12	22.38
j	2.98	37.15	33.74	18.93	7.20	26.13

Various samples of pure water and saline solutions: (a) DI water; (b) AuNT water; (c) sAuNT water; (d) DI water with 0.9 wt% NaCl; (e) AuNT water with 0.9% NaCl; (f) sAuNT water with 0.9% NaCl,; (g) AuNT water obtained without illumination of light; (h) Super sAuNT water: sAuNT water on supported Au NPs under in situ Raman experiment; (i) AgNT water obtained with illumination of green LED (maxima centered at 530 nm); (j) AgNT water obtained with illumination of blue LED (maxima centered at 460 nm).

Table S2 | Data from ESR spectra of hydroxyl free radicals based on various saline solutions, corresponding to Fig. S4.

	ESR intensity			
Samples	No. 1	No. 2	No. 3	Average
[a]DI water-NaCl	4000	3900	3750	3883±126
[b]AuNT water-NaCl	3500	3800	3500	3600±173
[c]sAuNT water-NaCl	3500	3250	3800	3517±275

Various samples of saline solutions: (a) DI water with 0.9 wt% NaCl; (b) AuNT water (illumination with fluorescent lamps in preparation) with 0.9% NaCl; (c) sAuNT water (illumination with green LED in preparation) with 0.9% NaCl.

References

1. Meyer, T. W. & Hostetter, T. H. Uremia. *N. Engl. J. Med*. **357**, 1316-1325 (2007).
2. Turi, S. *et al.* Oxidative stress and antioxidant defense mechanism in glomerular diseases. *Free Radical Biol. Med*. **22**, 161-168 (1997).
3. Herlebin, A., Nguyen, A. T., Zingraff, J., Urena, P. & Descamps-Latscha, B. Influence of uremia and hemodialysis on circulating interleukin-1 and tumor necrosis factor alpha. *Kidney Int*. **37**, 116-125 (1990).
4. Neelakandan, C. *et al.* In vitro evaluation of antioxidant and anti-inflammatory properties of genistein-modified hemodialysis membranes. *Biomacromolecules* **12**, 2447-2455 (2011).
5. Senthilkumar, S., Rajesh, S., Jayalakshmi, A. & Mohan, D. Biocompatibility studies of polyacrylonitrile membranes modified with carboxylated polyetherimide. *Mater. Sci. Eng. C* **33**, 3615-3626 (2013).
6. García-López, E., Lindholm, B. & Davies, S. An update on peritoneal dialysis solutions. *Nat. Rev. Nephrol.* **8**, 224-233 (2012).
7. Himmelfarb, J. & Alplkizler, T. Hemodialysis. *N. Engl. J. Med*. **363**, 1833-1845 (2010).
8. Chaban, V. V. & Prezhdo, O. V. Water boiling inside carbon nanotubes: toward efficient drug release. *ACS Nano* **5**, 5647-5655 (2011).
9. Hummer, G. Rasalah, J. C. & Noworyta, J. P. Water conduction through the hydrophobic channel of a carbon nanotube. *Nature* **414**, 188-190 (2001).
10. Humes, H. D., Buffington, D. A., MacKay, S. M., Funke, A. J. & Weitzel, W. F. Replacement of renal function in uremic animals with a tissue-engineered kidney. *Nat. Biotech*. **17**, 451-455 (1999).
11. Held, P. J., Levin, N. W., Bovbjerg, R. R., Pauly, M. V. & Diamond, L. H. Mortality and duration of hemodialysis treatment. *J. Am. Med. Assoc*. **265**, 871-875 (1997).
12. Marshall, M. R., Byrne, B. G., Kerr, P. G., Mc-Donald, S. P. Associations of hemodialysis dose and session length with mortality risk in Australian and New Zealand patients. *Kidney Int*. **69**, 1229-1236 (2006).
13. Himmelfarb, J. & Kliger, A. S. End-stage renal disease measures of quality. *Annu. Rev. Med*. **58**, 387-399 (2007).
14. Paladini, F., Pollini, M., Tala, A., Alifano, P. & Sannino, A. Efficacy of silver treated catheters for haemodialysis in preventing bacterial adhesion. *J. Mater. Sci: Mater Med*. **23**, 1983-1990 (2012).
15. Pollini, M. *et al.* Antibacterial coatings on haemodialysis catheters by

photochemical deposition of silver nanoparticles. *J. Mater. Sci: Mater Med*. **22**, 2005-2012 (2011).

16. Xia, S., Hodge, N., Laski, M. & Wiesner, T. F. Middle-molecule uremic toxin removal via hemodialysis augmented with an immunosorbent packed bed. *Ind. Eng. Chem. Res*. **49**, 1359-1369 (2010).
17. Ireland, R. Does reducing dialysate sodium level lower blood pressure? *Nat. Rev. Nephrol*. **8**, 192-192 (2012).
18. Damasiewicz, M. J., Polkinghorne, K. R. & Kerr, P. G. Water quality in conventional and home haemodialysis. *Nat. Rev. Nephrol*. **8**, 725-734 (2012).
19. Li, J. F. *et al.* Shell-isolated nanoparticle-enhanced Raman spectroscopy. *Nature* **464**, 392-395 (2010).
20. Tsai, M. F. *et al.* Au nanorod design as light-absorber in the first and second biological near-infrared windows for in vivo photothermal therapy. *ACS Nano* **7**, 5330-5342 (2013).
21. Yoshida, H. *et al.* Visualizing gas molecules interacting with supported nanoparticulate catalysts at reaction conditions. *Science* **335**, 317-319 (2012).
22. Neumann, O. *et al*. Solar vapor generation enabled by nanoparticles. *ACS Nano* **7**, 42-49 (2013).
23. Fang, Z. *et al*. Evolution of light-induced vapor generation at a liquid-immersed metallic nanoparticle. *Nano Lett.* **13**, 1736-1742 (2013).
24. David, J. G., Gierszal, K. P., Wang, P. & Ben-Amotz, D. Water structural transformation at molecular hydrophobic interfaces. *Nature* **491**, 582-585 (2012).
25. Li, R., Jiang, Z., Guan, Y., Yang, H. & Liu, B. Effects of metal ion on the water structure studied by the Raman O[BOND]H stretching spectrum. *J. Raman Spectrosc*. **40**, 1200-1204 (2009).
26. Carey, D. M. & Korenowski, G. M. Measurement of the Raman spectrum of liquid water. *J. Chem. Phys*. **108**, 2669-2775 (1998).
27. Tomlinson-Phillips, J., Davis, J. & Ben-Amotz, D. Structure and dynamics of water dangling OH bonds in hydrophobic hydration shells. Comparison of simulation and experiment. *J. Phys. Chem. A* **115**, 6177-6183 (2011).
28. Leberman, R. & Soper, A. K. Effect of high salt concentrations on water structure. *Nature* **378**, 364-366 (1995).
29. Chumaevskii, N. A., Rodnikova, M. N. & Sirotkin, D. A. Cationic effect in aqueous solutions of 1:1 electrolytes by Raman spectral data. *J. Mol. Liq*. **91**, 81-91 (2001).
30. Imlay, J. A. Cellular defenses against superoxide and hydrogen peroxide. *Annu. Rev. Biochem*. **77**, 755-756 (2008).

31. Lee, T. S. & Chau, L. Y. Heme oxygenase-1 mediates the anti-inflammatory effect of interleukin-10 in mice. *Nat. Med*. **8**, 240-246 (2002).
32. Meng, X. L. *et al*. RV09, a novel resveratrol analogue, inhibits NO and TNF-α production by LPS-activated microglia. *Int. Immunopharmacol*. **8**, 1074-1082 (2008).
33. Yu, C. C., Liu, Y. C., Yang, K. H. & Tsai, H. Y. Simple method to prepare size-controllable gold nanoparticles in solutions and their applications on surface-enhanced Raman scattering. *J. Raman Spectrosc*. **42**, 621-625 (2011).
34. Sun, Q. Raman spectroscopic study of the effects of dissolved NaCl on water structure. *Vib. Spectrosc*. **62**, 110-114 (2012).
35. Liu, Y. C., Yu, C. C. & Yang, K. H. Active catalysts of electrochemically prepared gold nanoparticles for the decomposition of aldehyde in alcohol solutions. *Electrochem. Commun*. **8**, 1163-1167 (2006).
36. Ohsawa, I. *et al*. Hydrogen acts as a therapeutic antioxidant by selectively reducing cytotoxic oxygen radicals. *Nat. Med*. **13**, 688-694 (2007).
37. Liu, Y. & Imlay, J. A. Cell death from antibiotics without the involvement of reactive oxygen species. *Science* **339**, 1210-1213 (2013).
38. Lin, H. C. *et al*. Structure–activity relationship of coumarin derivatives on xanthine oxidase-inhibiting and free radical-scavenging activities. *Biochem. Pharmacol*. **75**, 1416-1425 (2008).
39. Senior, W. A. & Thompson, W. K. Assignment of infra-red and Raman bands of liquid water. *Nature* **205**, 170-170 (1965).
40. Polman A. Solar steam nanobubbles. *ACS Nano* **7**, 15-18 (2013).
41. Remes, A. *et al.* Electrochemical determination of pentachlorophenol in water on a multi-wall carbon nanotubes-epoxy composite electrode. *Sensors* **12**, 7033-7046 (2012).
42. Dawson, A. & Kamat, P. V. Semiconductor−metal nanocomposites. Photoinduced fusion and photocatalysis of gold-capped TiO_2 (TiO_2/Gold) nanoparticles. *J. Phys. Chem. B* **105**, 960-966 (2001).
43. Vohringer-Martinez, E. *et al.* Water catalysis of a radical-molecule gas-phase reaction. *Science* **315**, 497-501 (2007).
44. Hammer, N. I. *et al*. How do small water clusters bind an excess electron? *Science* **306**, 675-679 (2004).
45. Ohshima, Y., Sato, K., Sumiyoshi, Y. & Endo, Y. Rotational spectrum and hydrogen bonding of the H_2O−HO radical complex. *J. Am. Chem. Soc.* **127**, 1108-1109 (2005).

46. Allodi, M. A., Dunn, M. E., Livada, J., Kirschner, K. N. & Shields, G. C. Do hydroxyl radical-water clusters, $OH(H_2O)n$, n=1-5, exist in the atmosphere? *J. Phys. Chem. A* **110**, 13283-13289 (2006).
47. Sohal, R. S. & Weindruch, R. Oxidative stress, caloric restriction, and aging. *Science* **273**, 59-63 (1996).